energies

Review

Under-Expanded Jets in Advanced Propulsion Systems—A Review of Latest Theoretical and Experimental Research Activities

Francesco Duronio [1], Carlo Villante [1,*] and Angelo De Vita [1,2]

[1] Department of Industrial Engineering, Information and Economics, Università degli Studi dell'Aquila, Piazzale Ernesto Pontieri, Monteluco di Roio, 67100 L'Aquila, Italy; francesco.duronio@univaq.it (F.D.); angelo.devita@univaq.it (A.D.V.)
[2] Consiglio Nazionale delle Ricerche, Istituto di Scienze e Tecnologie per l'Energia e la Mobilità Sostenibili (STEMS), Via G. Marconi 4, 80125 Napoli, Italy
* Correspondence: carlo.villante@univaq.it; Tel.: +39-0862434302

Abstract: The current ongoing rise in environmental pollution is leading research efforts toward the adoption of propulsion systems powered by gaseous fuels like hydrogen, methane, e-fuels, etc. Although gaseous fuels have been used in several types of propulsion systems, there are still many aspects that can be improved and require further study. For this reason, we considered it important to provide a review of the latest research topics, with a particular focus on the injection process. In advanced engine systems, fuel supply is achieved via enhanced direct injection into the combustion chamber. The latter involves the presence of under-expanded jets. Under-expanded jets are a particular kind of compressible flow. For this reason, the review initially provides a brief physical explanation of them. Next, experimental and numerical CFD investigation techniques are discussed. The last section of this manuscript presents an analysis of the jet's structure. The injection parameters commonly used are examined; next, the characteristics of the near-nozzle field are reviewed and finally, the far-field turbulent mixing, which strongly affects the air–fuel mixture formation process, is discussed.

Keywords: under-expanded; CFD; compressible flow; supersonic flow; gaseous injection

check for updates

Citation: Duronio, F.; Villante, C.; De Vita, A. Under-Expanded Jets in Advanced Propulsion Systems—A Review of Latest Theoretical and Experimental Research Activities. *Energies* **2023**, *16*, 6471. https://doi.org/10.3390/en16186471

Academic Editors: Vasily Novozhilov and Cunlu Zhao

Received: 29 July 2023
Revised: 27 August 2023
Accepted: 4 September 2023
Published: 7 September 2023

Copyright: © 2023 by the authors. Licensee MDPI, Basel, Switzerland. This article is an open access article distributed under the terms and conditions of the Creative Commons Attribution (CC BY) license (https://creativecommons.org/licenses/by/4.0/).

1. Introduction

One of the essential actions for mitigating current climate change risks is to significantly reduce transport sector emissions [1–4]. As a consequence, over the last few years, an increasing number of researchers have focused on the development of advanced propulsion systems [5]. In particular, powering Internal Combustion engines (ICEs) with gaseous or strong evaporative fuels (like hydrogen, propane or methane gas) may be introduced in the near future and also maintained for a longer period (especially if equipping heavy-duty long-range transport applications) to achieve the aforementioned goal [6]. Furthermore, these fuels may also be completely renewable and/or have zero emissions on a WTW (well-to-wheel) evaluation approach, therefore leading to zero-impact transportation solutions to be compared with all those based on pure electric traction [7].

When using gaseous fuels, the injection process plays the most crucial role in defining ICE environmental performance, affecting mixture formation, its combustion, and, therefore, production of pollution. Moreover, in advanced ICEs, the fuel is Directly Injected (DI) inside the cylinder, calling for more rapid, controlled and efficient mixture formation processes [8–10].

High-injection pressures are typically used for gaseous fuelling in order to achieve the required mass flow rates and promote air/fuel mixing [11–17], typically leading to the formation of highly under-expanded jets (UEJ) at the injector outlet, when the fuel jet faces surrounding airflow.

Under-expanded jets are complex high-speed flows, which are also formed in many other engineering applications and devices such as exhaust aircraft plumes (rockets and missiles), supersonic combustion chambers, actuators, etc. [18–20]. This type of jet can also be observed in geophysical systems (volcanic eruption) and in the accidental release of hazardous gases (such as hydrogen) from tiny cracks in high-pressure pipelines and reservoirs [21–23]. For these reasons, under-expanded jets were historically investigated, especially for aerospace applications. At the same time, there are a paucity of studies examining their presence and influence in automotive advanced propulsion systems, being a newer topic in fluid-dynamic and engine-related research.

However, in recent years, following the great interest shown by political institutions in fuels like hydrogen, a multitude of scientific studies were conducted [24–28]. The authors propose that it could be important to provide researchers with a quick and, as far as possible, complete reference guide to under-expanded jets in ICEs, highlighting the most interesting topics and the most relevant works undertaken in recent years.

To this aim, this review paper firstly focuses on a brief physical and phenomenological discussion of these complex flows and then reports on the main literature results in the sector, subsequently dividing them into two main sections concerning, respectively, experimental and mathematical investigation methodologies usually adopted for studying UEJ. Each cited research study will be introduced and briefly discussed, highlighting the most important outcomes from a fluid-dynamic perspective and final engine application.

2. Physics of Under-Expanded Jets

An under-expanded jet may appear when a high-pressure fluid is connected through a convergent or a convergent–divergent nozzle within an environment where much lower pressure conditions are created. As well known, two possible scenarios can be identified depending on the total pressure ratio between the inlet and outlet of the nozzle.

$$\eta_0 = \frac{P_0}{P_\infty} \tag{1}$$

Figures 1 and 2 report the pressure ratio and the mass flow rate evolution as a function of the axial distance for a convergent nozzle.

The first regime depicts a subsonic flow (cases a and b); the mass flow increases as the downstream pressure decreases, and the exit pressure is equal to the ambient one. Critical conditions are reached if the upstream pressure increases and the nozzle is choked (cases c and d). The outflow pressure is equal to the critical pressure (P^*), and the mass flow cannot increase more; it is called indeed choked as reported in Figure 2.

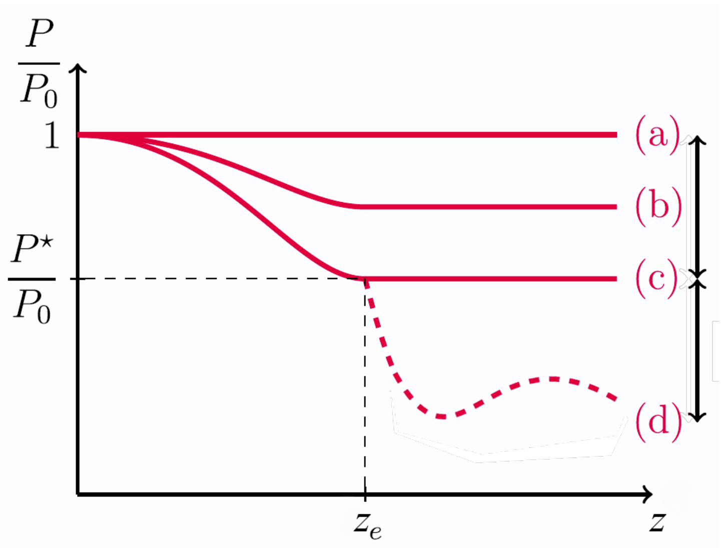

Figure 1. Pressure evolution along nozzle axis for various pressure ratios.

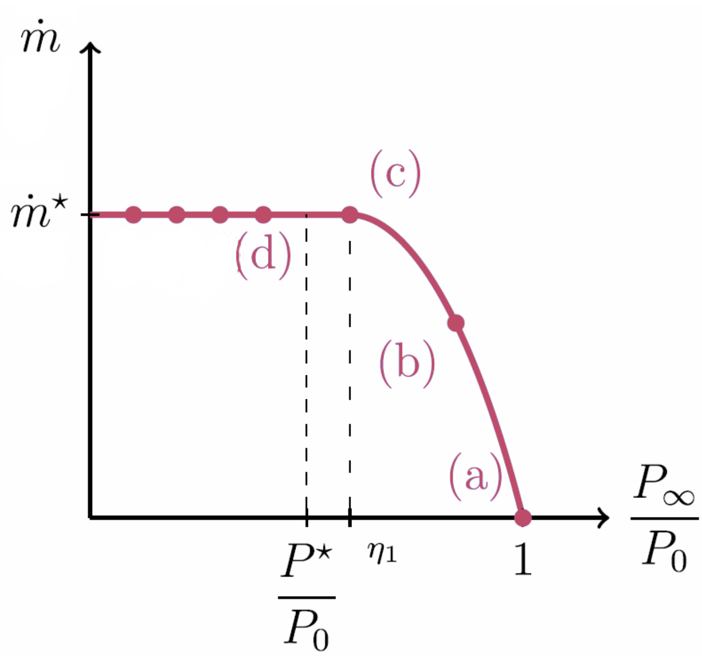

Figure 2. Mass flow rate for various pressure ratios.

It follows that, an the exit section, the pressure is greater than the ambient one and to achieve pressure equilibrium, under-expanded jets arise.

In choked conditions, the pressure waves cannot travel back upstream, and the mass flow rate is no longer dependent on downstream conditions ($\dot{m}^*$). The flow characteristics inside the nozzle, in fact, only depend only on the upstream boundary conditions.

As represented in Figure 3, it is common practice to divide the jet into three zones [29]:

- the near-nozzle zone;
- the transition zone;
- the far-field zone;

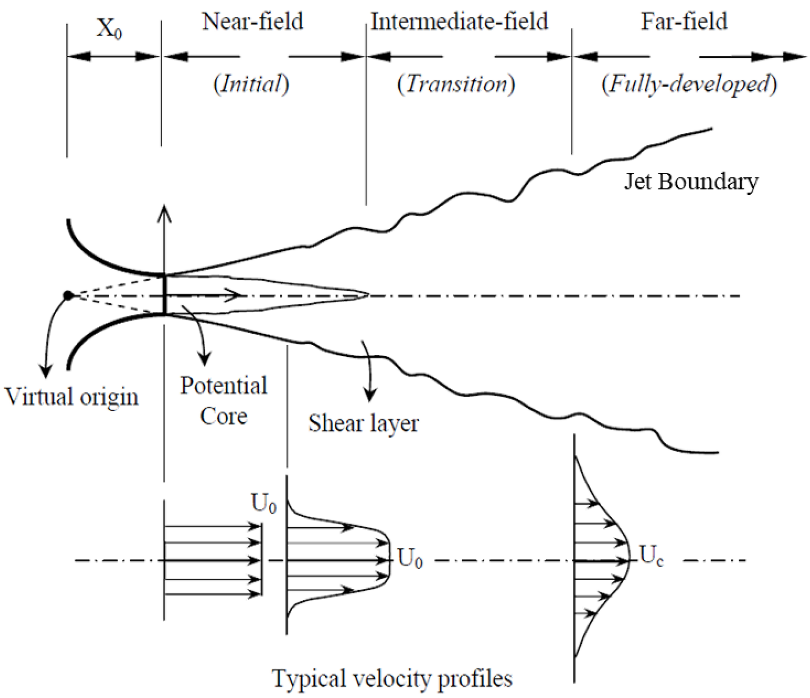

Figure 3. Under-expanded jet zones.

The near-nozzle zone is split into two sections: the core and the mixing layer. In the former, also called the gas-dynamic area, the flow is separated from the environment, and its behaviour is governed mostly by compressible effects and is rather steady. The fluid expands iso-entropically until it is re-compressed by shock waves.

In the mixing layer, turbulence causes an interaction between the injected fluid and the surrounding environment, which is characterized by huge turbulent structures (vortices) that are formed within the fluid flow downstream of the nozzle outlet. A shearing zone between the frontier of the potential core of the jet and the constant pressure line can be distinguished.

Depending on the pressure ratio, different under-expanded jet configurations can be observed in the near-nozzle zone:

- The jet is weakly under-expanded, a normal shock appears in the exit plane.
- The jet is moderately under-expanded and has a "diamond" or "X" structure, depicted in Figure 4, $2 < \eta_0 < 4$ [30,31]. In the exit plane (marker A), a Prandtl–Meyer expansion fan (marker C) expands the fluid downstream of the device's edges up to the jet boundary that corresponds to the external surface of the mixing layer (marked JB). The expansion waves are reflected as compression waves when they reach the constant pressure streamline (marker D), where the pressure matches the ambient pressure. They converge on the inner jet and merge to produce an oblique shock (marker E), commonly referred to as the intercepting shock.
- The jet is highly under-expanded, $4 < \eta_0 < 7$ [32,33]. It has a "barrel" or "bottle" structure, shown in Figure 5, Mach disc appears (due to a singular reflection). When the pressure ratio grows, the regular reflection of the intercepting shock on the axis is no longer possible. As a result, above the critical angle, this reflection becomes singular, resulting in the appearance of a normal shock-denominated Mach disc (marker F). The triple point is defined as the intersection of the intercepting shock, the Mach disc and the reflected shock (marker G). A slipstream (marker H) develops at this point: this is an embedded shear layer that divides the flow upstream of the Mach disc (subsonic) from the flow downstream of the reflected shock (supersonic).
- The jet is extremely (or very highly) under-expanded, $\eta_0 > 7$ [34,35]. As depicted in Figure 6, the structure is dominated by a unique barrel. In this case, the Mach disc is no longer considered as a normal shock, and its curvature must be considered. Due to the momentum exchange generated by the ambient fluid's entrainment, the jet's overall diameter will decrease, resulting in an extremely long plume.

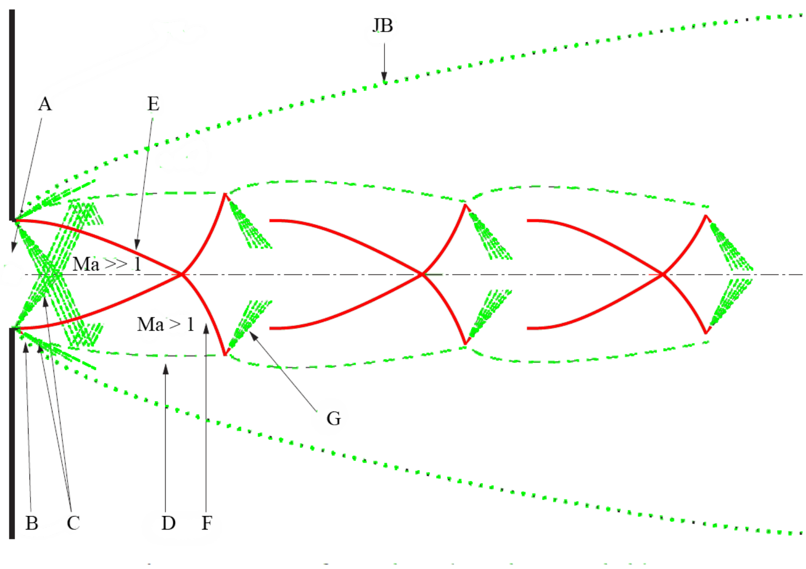

Figure 4. Structure of a moderately under-expanded jet.

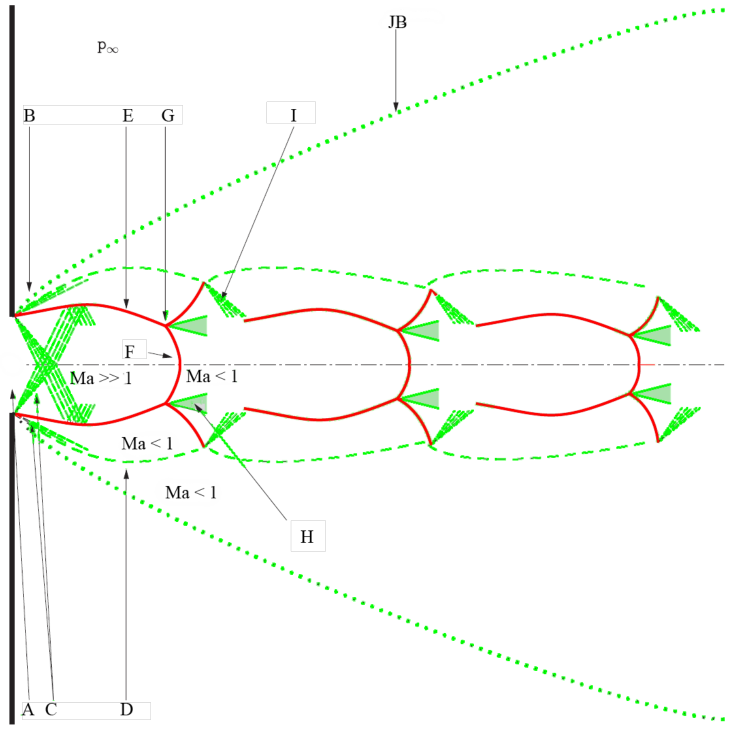

Figure 5. Structure of a highly under-expanded jet.

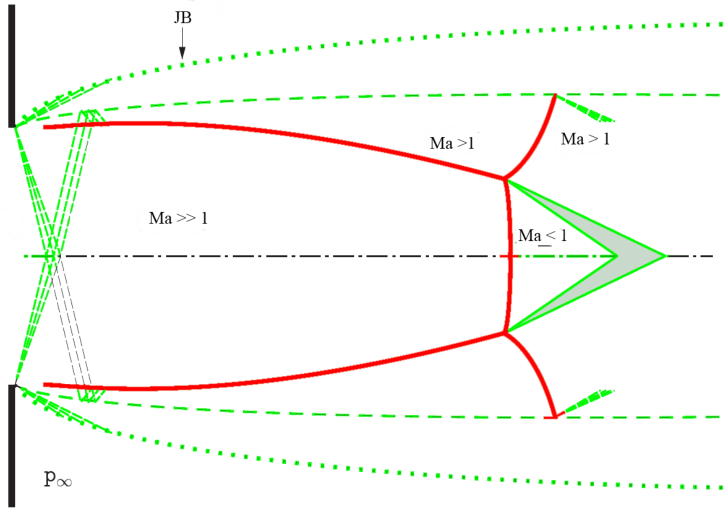

Figure 6. Structure of a very highly under-expanded jet.

Nevertheless, the Mach disc is undoubtedly one of the most studied features of under-expanded jets Moreover, there is still significant ongoing discussion regarding the transition from a regular reflection to a singular reflection, accompanied by the appearance of the Mach disc. This phenomenon is currently quantitatively not well known, particularly the dependence (and interactions) on pressure range and exit Mach number, fluid characteristics (i.e., the polytropic coefficient), nozzle shape, and exit nozzle angle [36].

The Mach disc location is primarily governed by the pressure ratio, increases with the Mach number and, among the many, a good estimation of the position is given by the following relation:

$$\frac{H_d}{D} = 0.67\sqrt{\eta_0} \tag{2}$$

with H_d Mach disc height, D outlet section diameter [34,36,37].

The Mach disc width or diameter was clearly less investigated than the Mach disc length. However, it appears that it is also mainly governed by the pressure ratio and strongly dependent on the nozzle geometry and shape [38–40].

Towards the end of the near-nozzle zone, the sonic line reaches the axis, indicating that the mixing layer has fully replaced the inner region. This marks the beginning of the transition zone, where variations in variables, both longitudinally and radially, become minimal. In this region, a more effective mixing of the two fluids, the ejected fluid and the ambient fluid, takes place. As a result, the pressure field becomes more homogenized as entrainment occurs throughout the transition zone.

In the far-field zone, the jet exhibits self-similarity, but compressible effects may still be present if the Mach number is above 0.3 and may even be supersonic. Qualitatively, the normalized radial profiles of the mean variables follow the same pattern, typically characterized by a Gaussian profile.

3. Experimental Observation of Under-Expanded Jets

The observation of under-expanded jets can be performed both with quantitative and qualitative techniques. Among the first category, schlieren and shadowgraph imaging surely can be mentioned, adopted for capturing images of both near and far field zones [13,41–43].

High-speed schlieren imaging is a robust diagnostic technique capable of visualizing optical in-homogeneities of transparent media, otherwise not visible to the human eye [44–46]. The method is sensitive to changes in the refractive index of a light beam travelling through a heterogeneous medium. For this reason, Schlieren diagnostic is frequently adopted for the observation of compressible flows, such as under-expanded jets, in which the difference in refractive index is caused by the gradient of density between the injected fuel and the ambient gas [44].

Figure 7 shows the schematic diagram of a typical experimental setup for schlieren imaging.

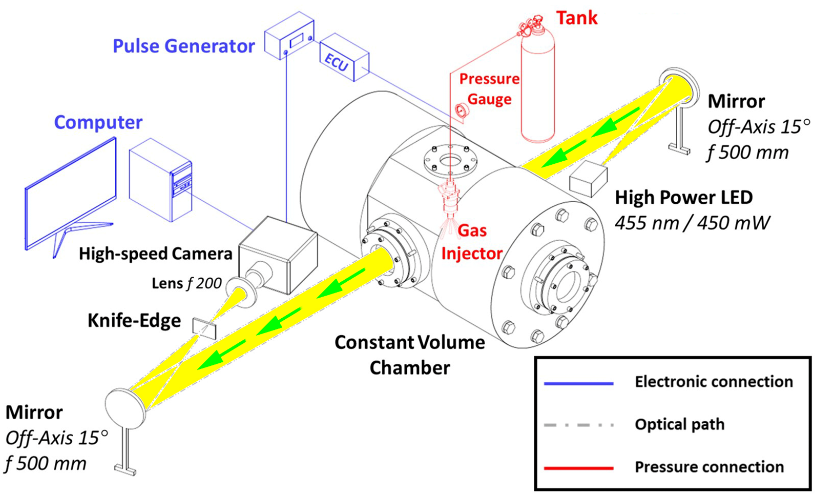

Figure 7. Experimental optical setup of schlieren technique with z-type configuration (reproduced with permission from Ref. [47]. Copyright 2020 SAE International).

The Schlieren light source is usually a high-power LED lamp. A series of lenses and glasses modify the beam characteristics. The main difference between Schlieren and shadowgraph is the presence of a knife-edge in the first case to regulate the percent of light cutoff, obtaining the desired contrast for the Schlieren images. High-speed cameras are adopted for recording images with frame rates of the order of thousands of frames per second. Depending on the magnification system, different spatial resolutions can be achieved.

The injection system usually consists of a pressurized fuel tank, a pressure transducer and a pressure regulator to ensure the desired value for the test conditions. The transistor–transistor logic (TTL) triggering signal produced by a pulse generator is used by an Electronic Control Unit (ECU) to control the injection events and to guarantee proper synchronization and delay between the injection and acquisition chain.

Under-expanded jets are almost always being observed in Constant Volume Chambers (CVC), optically accessible through quartz windows with the injector fixed in a customized holder.

The images recorded with these techniques provide a proficient visualization of the near field zone, and so of the barrel shocks, the Mach discs, etc., as well as the overall spray structure, allowing the evaluation of macroscopic parameters such as the Mach disc height, width, the jet tip penetration, the jet angle, the volumetric growth, the tip speed, radial expansion, etc. Figure 8 depicts some classical visualization of the under-expanded jets obtained with schlieren imaging and regarding various jet's characteristics [48].

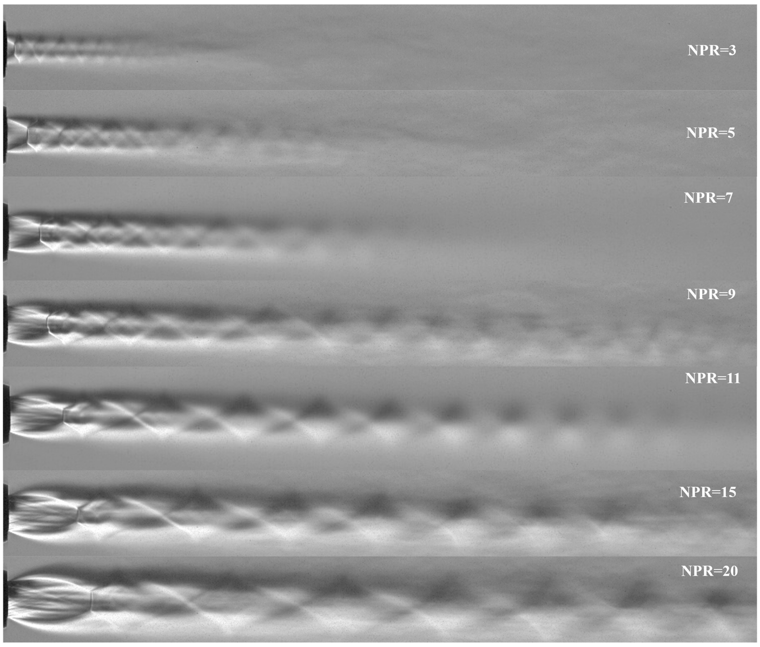

Figure 8. Visualization of under-expanded jets by means of schlieren optical technique (reproduced with permission from Ref. [48]. Copyright 2022 Elsevier).

These information are of relevant importance for verifying and validating CFD simulation codes by comparison of the aforementioned parameters but, at the same time, do not allow to evaluate microscopic features of the jet or give a quantitative estimation of local fuel concentration, jet temperature or velocity. To obtain some of these information other experimental techniques are required. They are Planar Laser-Induced Fluorescence (PLIF) or Particle Image Velocimetry (PIV) [43,49–53].

The PIV technique is a non-intrusive diagnostic technique that allows the velocity field to be measured on a two-dimensional plane. The measurement principle is based on determining the distance the tracer particles cover in a known time interval [54,55]. The typical elements of a PIV system are a laser source (typically a pulsed Nd-YAG laser with a wavelength of 532 nm), an optical system, a camera and a data acquisition system (DAQ).

The PLIF technique allows the measurement of the concentration of species and the temperature in the flow field of a fluid. It is based on the process of photon absorption–emission, and therefore, on the phenomenon of natural fluorescence of molecules and atoms. Through the PLIF technique, it is possible to obtain visualization with high spatio-temporal resolution. Although the instantaneous (temporally based) quantitative measurement of the parameters of interest remains complex, it is still possible to obtain quantitative measurements of concentration, temperature, pressure and speed based on an average of consecutive sequences (time-averaged).

Figure 9 depicts some results regarding the fuel concentration of under-expanded jets [53].

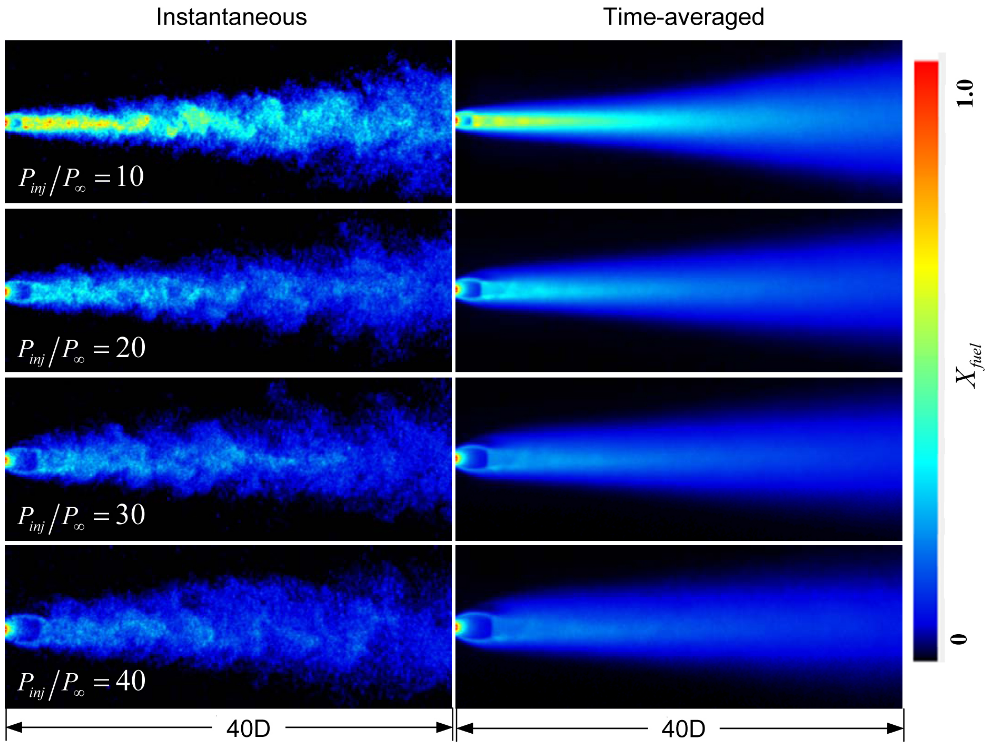

Figure 9. Visualization of under-expanded jets by means of PLIF optical technique for different P_{inj}/P_{amb} ratios (reproduced with permission from Ref. [53]. Copyright 2013 SAE International).

Table 1 summarizes the papers regarding experimental investigations of under-expanded jets.

Table 1. Experimental Techniques Jets Summary Table.

Technique	Measurement Zone	Fuel	NPR	Reference
Schlieren	Developed Spray	CH_4	$P_{inj} = 300$ bar $P_{amb} = 60, 12, 30$ bar	[56]
	Developed Spray	He	$NPR = 2, 3, 4, 5$	[13]
	Near-nozzle/ Mach Disc	N_2	$NPR = 20$	[57]
	Developed Spray	CH_4	NPR = 190, 220, 250, 280, 310	[43]
	Developed Spray	CH_4	$NPR = 60, 11, 16, 21, 26$	[41]
	Developed Spray	CH_4	$P_{inj} = 10, 14, 18$ bar $P_{amb} = 3, 5$ bar	[42]
PLIF	Near-nozzle/Mach Disc	N_2	$NPR = 10, 20, 30, 40$	[50]
	Developed Spray	N_2	$NPR = 10, 40$	[53]
	Developed Spray	CH_4	$NPR = 20, 60$	[51]
PIV	Developed Spray	N_2	$NPR = 20$	[57]
	Developed Spray	Ar	$NPR = 12$	[58]

4. CFD Simulation of Under-Expanded Jets

Computational fluid dynamic codes (CFD) are undoubtedly the other powerful tool broadly adopted to investigate under-expanded jets. The advantages of developing a virtual model of this engineering problem are quite obvious not only to understand the underlying physics of these flows but also with the perspective of the application to the propulsion system.

This paragraph aims to illustrate, in a synthetic but also organized fashion, the main characteristics of the CFD codes used by researchers to study the aforementioned problem. Further than in-house developed codes, basically three finite volume CFD codes were used. They are OpenFOAM, CONVERGE and STAR-CCM+ [59–61]. It should also be mentioned that some studies use the Lattice Boltzmann method [62,63]. The following two sub-sections report the main characteristics of the discretization schemes adopted and of the turbulence modelling selected.

4.1. Discretization Schemes and Solution Algorithms

The simulation of under-expanded jets requires the adoption of high-order numerical schemes able to describe flow-field discontinuities along with avoiding undesired oscillations. High-order schemes are required both for spatial discretization and temporal integration.

Methodologies, based on Riemann solvers, such as the Weighted Essentially Non-Oscillatory schemes (WENO) or the Piecewise Parabolic Method (PPM), give the best reproduction of compressible flow but have relevant limitations. These approaches involve characteristic decomposition and Jacobian evaluation, and so they were implemented only for structured grids. The adaptive central-upwind sixth-order weighted essentially non-oscillatory (WENO-CU6) scheme with low dissipation was used by Ren Z et al. [64] to achieve a proper resolution of the flow properties around the shock waves. Seventh-order accurate weighted essentially non-oscillatory (WENO7) reconstruction of the characteristic fluxes was also adopted for simulating under-expanded jets. The shocks and discontinuities can be resolved using highly accurate and low-dissipation hybrid ENO schemes with shock detectors [65–67].

Contrarily, unstructured grids are far more flexible than structured grids and can easily discretize complex geometries [68–70]. One of the principal methods developed for unstructured grids uses the so-called central schemes formulations of Kurganov (KNP) and Kurganov and Tadmor (KT) [71,72]. These are non-staggered second-order central methods that use the cell centres' values to evaluate the cell faces' fluxes. The cell-to-face flow interpolation is divided into inward and outward directions with respect to the face owner cell. An extensive and detailed description can be found in [68]. Considering the intrinsic geometrical complexity of the injector's nozzles, these schemes are broadly adopted for this kind of simulation in union with flux limiters of Minmod or of Van Leer to ensure stability and convergence of the computation [68,73]. This discretization method, initially implemented in OpenFOAM's solver *rhoCentralFoam*, was exploited in various other solvers purposely developed to study under-expanded jets [74–80]. Another proficient scheme used is the Advection Upstream Splitting Method (AUSM$^+$-up). AUSM+-up is accurate and reliable in solving fluid flows with any arbitrary range of velocities, but it excels at high-velocity flows with strong discontinuities like shock waves [81,82]. AUSM+-up avoids explicit artificial dissipation by using a separate splitting for the pressure terms of the governing equations; the mass flux and pressure flux are calculated on the basis of local flow characteristics (including the speed of sound) to ensure precise information propagation inside the fluid for convective and acoustic processes [83]. This minimizes numerical dissipation, especially in high-velocity flows, and prevents wiggles at flow discontinuities like shocks.

The solution methods commonly used involve both explicit (density-based) [84–86] and Pressure Implicit Split Operator (PISO) algorithms [56,87–90]. The density-based approach proved to be the best choice for reproducing under-expanded jet features. Implicit (or pressure-based) methods for solving fluid-flow governing equations were historically employed for incompressible flows and only recently adapted to account for compressible flows. However, as broadly demonstrated in the literature [84–86,89], the best choice in terms of results accuracy is represented by explicit methods (or density-based). The reason for that is intrinsically contained in the algorithm procedure. The temporal integration is usually performed using high-order schemes such as explicit Runge–Kutta 4th (RK4) [84].

Another relevant aspect of under-expanded jet simulation is the computation of the thermo-physical properties for the species involved in the fluid flow. The equation of state (EoS) (for a description of the pressure–volume–temperature (P-V-T) relationship) is crucial to the accuracy of the solution. Further than the ideal-gas EoS, Cubic EoS such as Soave–Redlich–Kwong (SRK) and Peng–Robinson (PR) were widely applied due to their simplicity and reasonable accuracy [56,61,76,77,91–94].

4.2. Turbulence Modelling

The numerical solution of the fluid-dynamic problem is valid when the computational grid is fine enough to resolve all the flow scales [85]. This would be a Direct Numerical Simulation (DNS) of the flow, which is now unaffordable due to its complexity and resource demands. So, turbulence modelling techniques, such as Reynolds Averaged Navier Stokes (RANS) or Large Eddy Simulation (LES), are preferred for under-expanded jet simulations [78,85,86,95].

Among the many simulation approaches regarding under-expanded jets, just a few use RANS, while most adopt LES models. The LES technique is based on modelling the lower scales, which are universal and unaffected by flow geometry, while explicitly solving the larger ones. This is done by mathematically filtering the governing equations and introducing the Sub-Grid Stress (SGS) tensor (τ_{sgs}) [96]. The SGS term modelling involves an eddy viscosity approximation. Various SGS closure models can be found in the literature. In some cases, LES WALE model is used, both without wall functions or applying global damping functions. The model produces an efficient and fast-solving scheme due to its algebraic formulation. This approach also showed some promising results in predicting the transition from laminar to turbulent regimes [97].

The Yoshizawa model is another common choice. It is a one-equation eddy viscosity model for compressible flows [98,99], which is different from zero equation models such as the Smagorisky model. It exploits a transport equation to compute the local SGS kinetic energy k_{sgs}. Then, the sub-grid scale eddy viscosity ν_{sgs} is calculated using the k_{sgs} field and the filter dimension Δ (usually evaluated from the grid size) according to the following relation:

$$\nu_{sgs} = C_k \Delta \sqrt{k_{sgs}} \tag{3}$$

where C_k is a model constant whose default value is 0.094.

The scale selective discretization (SSD) technique proposed by Vuorinen et al. relates to the so-called implicit LES (ILES) modelling category [84,100–102]. However, unlike ILES, the SSD approach targets the dissipative effects exclusively to the flow's smallest scales via scale separation procedure. A Laplacian filter separates the scales by splitting the convection term into low and high-frequency components for which centred and upwind-biased techniques can be used individually.

Table 2 summarizes the papers regarding CFD simulations of under-expanded jets.

Table 2. CFD Simulations Summary Table.

Numerical Approach	Code	Turbulence Modeling	Fuel	Reference
WENO/ENO	In-house	LES	Air	[65]
	In-house	LES	Air	[66]
	In-house/Finite Differences	LES	Reactive jet	[67]
	In-house	LES	H_2	[64]
AUSM	STAR CCM+	LES WALE	H_2	[60,82,89,103]
		LES WALE	N_2	[60,103]
		LES WALE	CH_4	[89,103]

Table 2. *Cont.*

Numerical Approach	Code	Turbulence Modeling	Fuel	Reference
KNP/KT	OpenFOAM OpenFOAM OpenFOAM	LES, RANS k-ω LES k-Eqn LES k-Eqn	H_2 N_2 CH_4	[74,86] [77,86] [47,75,104,105]
Bulk Viscosity Method	OpenFOAM	LES Scale Selective Method	N_2 CH_4 H_2	[53,85] [84] [53]
Hybrid KNP/KT	OpenFOAM OpenFOAM	LES LES, RANS	CH_4 H_2	[56,106,107] [61,108]
MUSCL	CONVERGE	LES	CH_4	[61,109]
Lattice Boltzmann	In-house	LES	N.A.	[62,63]

5. Jet Structure Analysis

Although we are considering pure experimental research or a CFD investigation, the information provided can be classified and subdivided in the following paragraphs.

First of all, the main parameters of the injection process are reviewed and discussed; then, the features of the Mach discs and, generally, of the near field flow are presented accordingly with the outcomes of the works considered. Finally, the characterization of the turbulent mixing zone and of the far-field zone are discussed being of central importance in propulsion systems applications.

5.1. Characteristics and Parameters of the Injection

The injectors investigated in the literature are mainly single-hole prototype devices. These usually have round holes with a diameter of about 1 mm [41,60,78]. Some other authors investigated hollow cone outwardly opening devices [52,88,109,110]. One of these is produced by Continental (Figure 10), and it was characterized both numerically and experimentally.

Commercially available injectors were also modified to inject gaseous fuels generating multi-hole patterned sprays [13,43,57].

Very few works were found concerning multi-hole injectors purposely designed for gaseous injection. A 50 bar maximum injection pressure device with inter-changeable nozzles was investigated experimentally and numerically in a series of publications [104,105].

When working with gaseous injection, typically, Net Pressure Ratio (NPR), the ratio between the injection and the environment pressure, is conveniently used as a reference to classify the resulting jets, more so than using injection pressure. In particular, common NPR values range from 4 to 5 to around 40–50 [42,43,104]. The ambient pressure is usually kept equal to 1 bar. Some works explore injection pressures up to 200 bar [51].

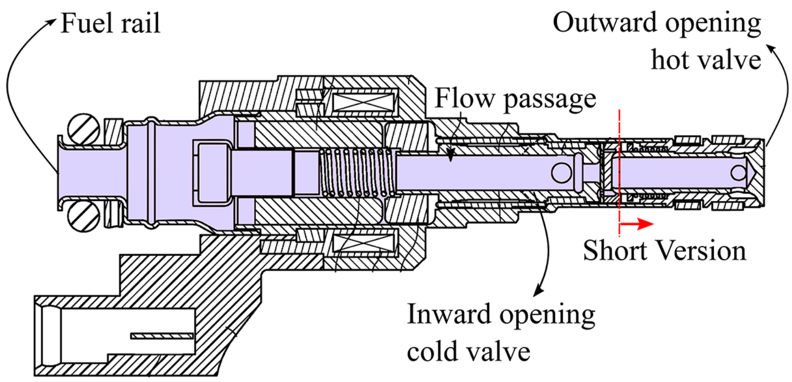

Figure 10. Outwardly opening injector for gaseous injections (reproduced with permission from Ref. [109]. Copyright 2020 The University of Queensland).

In the investigation of under-expanded jets, the characteristics of the injected fluid play a very important role, strongly influencing resulting jet conditions. However, due to security issues, experimental investigations are normally realized with inert gases like N2, argon or helium [52,58,92,111]. Moreover, some papers examine methane or hydrogen injections, the latter especially considering the latest interest in this fuel shown by many research groups. From the perspective of potential application in propulsion systems, testing inert gas is mainly used to validate and calibrate numerical CFD approaches, which can afterwards be extended to flammable fluid injections and mixture formation processes.

5.2. Near Field—Mach Disc Features

The investigation of the near nozzle flow field of under-expanded jets is mainly focused on Mach discs, barrel shocks or converging shocks that appear in this flow just downstream of the injector nozzle. Schlieren imaging is undoubtedly the most adopted technique to record them. The pictures obtained are a powerful tool to validate the CFD codes. Further than a visual comparison of the Schlieren measurements with the gradient of the density field computed with CFD, the Mach disc's height and width represent quantitative parameters that can be used for an actual comparison. An investigation using the PLIF technique was instead performed by Yu et al. [50]. The following Figure 11 depicts a comparison between LES simulation and PLIF visualization of the Mach disc issued from a methane injection.

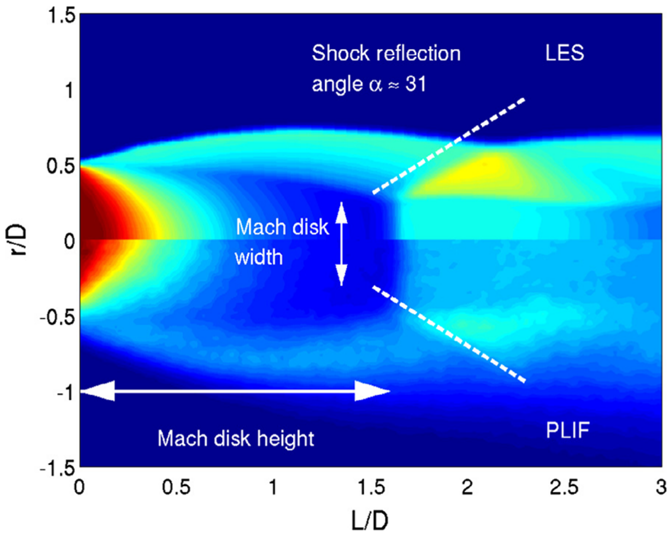

Figure 11. Mach disc: comparison of experimental PLIF images with LES CFD simulation (reproduced with permission from Ref. [50]. Copyright 2013 Elsevier).

The computational requirements for under-expanded jets simulations are very high. Grid sensitivity analysis performed by various authors demonstrated that to have a proficient representation of the near nozzle shocks mesh dimensions must be of the order of D/20–D/50 or, in dimensional terms, of tens of micro-meter [84,85,89,103]. This, together with the time step of the order of 10^{-8} s, requires relevant computational resources.

From a modelling point of view interesting comparisons between different CFD codes (such as OpenFOAM, Star CCM+ and CONVERGE) were carried out by various authors [61,112].

The equation of state was also investigated. Redwlich-Kwong and Peng-Robinson real gas EoS give different configurations of under-expanded jets with respect to ideal gas EoS especially when the jets are issued in critical conditions [106,107]. Other fluid properties, such as specific heat or viscosity are also objects of interest. Chung relation and Chapman–Enskog theory were used for the viscosity while the Janaf pressure-corrected relation for C_p and C_v [58,113].

The effect of the NPR on the characteristics of the Mach disc is one of the most investigated physical parameters demonstrating how, depending on the value assumed, the jet configuration significantly changes. Figure 12 shows the different shock structures obtainable accordingly with the net pressure ratio.

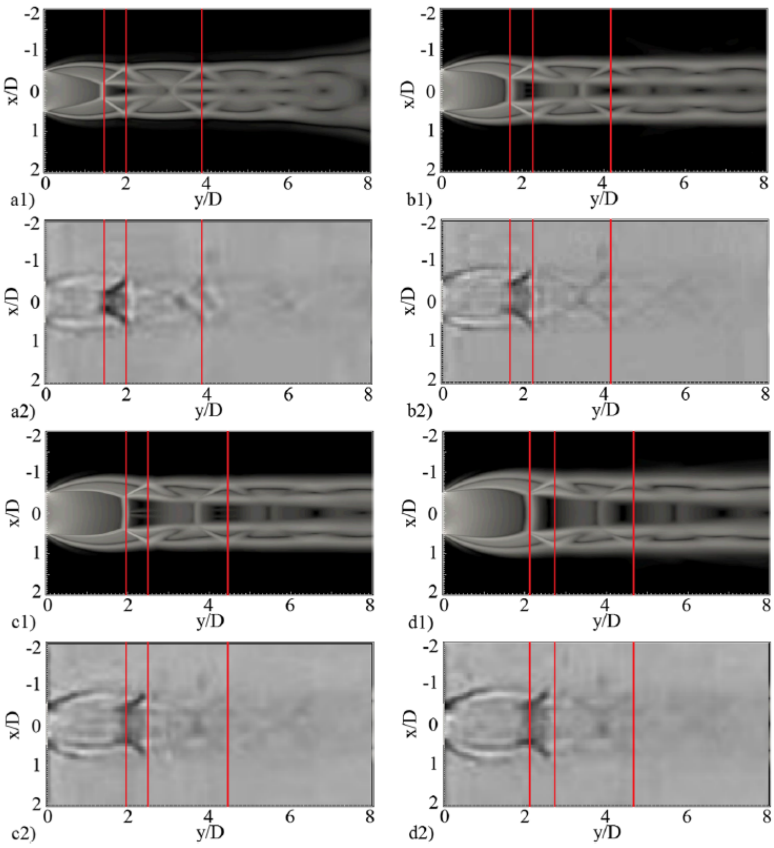

Figure 12. Mach discs: comparison of different pressure ratios. (**a1**,**a2**) NPR = 5.60, (**b1**,**b2**) NPR = 7.47, (**c1**,**c2**) NPR = 9.34, and (**d1**,**d2**) NPR = 11.2 (reproduced with permission from Ref. [77]. Copyright 2016 American Institute of Aeronautics and Astronautics).

The effect of the fuel characteristics was also an important research topic treated by Hamzehloo et al. comparing mach discs produced with hydrogen and methane [89,103]. The near-nozzle shock structure of the methane jet displayed a slightly different pattern compared to the hydrogen jets. The methane jet exhibited intense expansion fans right from the early stages of its formation, resulting in a normal shock that was wider than the nozzle diameter and resembled a Mach disc. On the other hand, the hydrogen jets were associated with a slim Mach disc. For methane, mixing occurs only downstream of the Mach disc while, for hydrogen, high momentum exchange and mixing was observed at the boundaries of the jet.

5.3. Far Field—Turbulent Mixing

Jet area, volumetric growth and tip penetration are the main parameters used to describe the characteristics of the far field and especially to validate the CFD approach exploiting schlieren images [43,53,56].

PLIF and PIV measurements also make it possible to characterize the mixing process, providing detailed information about the local fuel concentration and about the velocity field [49,53]. Axial and transverse density concentration profiles are also common plots produced from both simulation results and experimental measurements.

Two main approaches are used to characterize the mixing process: Scalar Dissipation Rate (SDR) and the development of a Probability density function (PDF).

The SDR is a measure of the mixing activity. Higher SDR values indicate more significant fuel concentration gradients. Low SDR values, on the other hand, indicate a very homogeneous spatial distribution of the fuel. This means that good mixing has already occurred (because the gradients have faded) or, even more, that no mixing is occurring.

The potential core of the jet, which extends averagely for 10/20 diameters downstream, is surrounded by a mixing layer where, in the radial direction, the fuel concentration decreases quickly. CFD simulations show that mixing does not occur in the central core where the jet is supersonic. Only downstream, when the flow becomes subsonic, turbulent air-fuel mixing begins. String-like structures highlight the edges between high and low-concentration regions.

Figure 13 reports an example of SDR computed for an under-expanded methane jet.

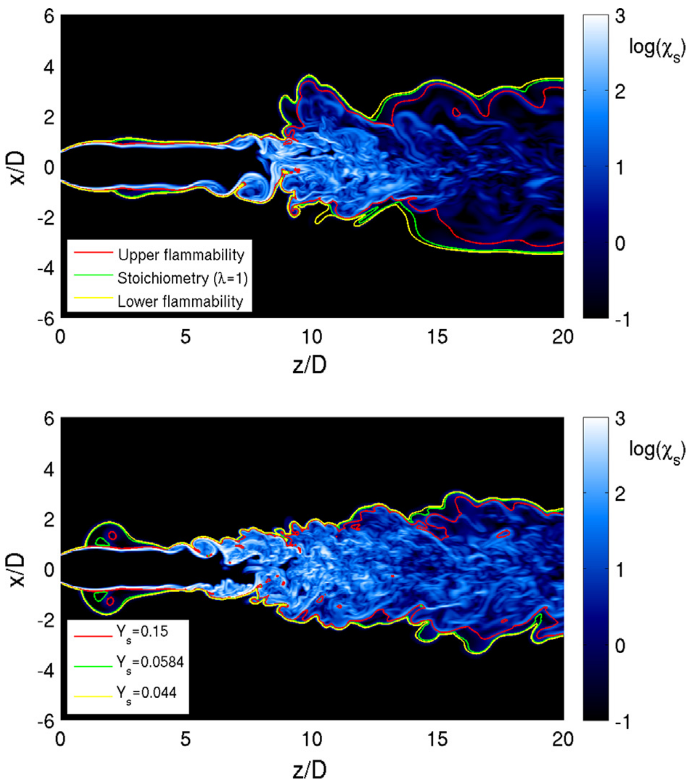

Figure 13. Scalar dissipation rate plot for two different injected fuels: N2 top and CH4 bottom. The isolines delimit zones where the fuel concentration is within the flammability limits or in stoichiometric conditions (reproduced with permission from Ref. [84]. Copyright 2014 Elsevier).

Some research used an SDR approach, concluding that a higher NPR favours a better and quicker air/fuel mixing [53,65,75]. This shows that NPR may substantially modify the mixing processes, which is not good news considering that high gaseous fuel injection pressures are typically not easily reachable due to intrinsic limitations in on-board gaseous fuel storage systems [114].

Achieving a quantitative estimation of the global mixture quality has relevant importance, especially with regard to the combustion process. Therefore, a statistical approach is commonly adopted to characterize the mixture obtained from the injection process. A mass-weighted probability density function (PDF) is usually calculated from the CFD results providing plots like the one in Figure 14.

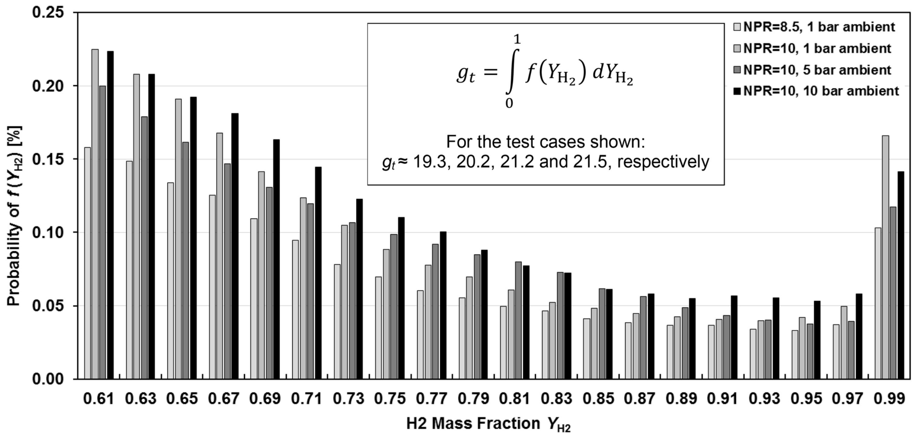

Figure 14. Probability density function computed to evaluate hydrogen mixture quality (reproduced with permission from Ref. [103]. Copyright 2016 Elsevier).

If the PDF function is integrated over different ranges of fuel concentration, it allows to estimate the percentage of lean, flammable and rich mixture [51,85,103]. This is important for evaluating the dynamics of the combustion process that follows the injection.

Turbulence effects are relevant in describing the structure of under-expanded jets far field. The common way to describe turbulence characteristics is to plot Q-criterion iso-surfaces or vorticity vectors; various authors did this on different kinds of jets [57,104,105].

Proper orthogonal decomposition (POD) was exploited by Vuorinen et al. [85] to project the turbulent flow field on basis functions that maximize the turbulent kinetic energy content for any subset of the base. The dominant structures indicate a helical mode and the spatial location and shown dynamics of the mode matches the previously existing picture of noise production.

The compressible vorticity transport equation rules vorticity evolution. Analysis of the driving forces to distort the streamwise vortices was performed by Li X et al. because it helps to understand the turbulent transition mechanisms [77]. The authors demonstrated that the dilatational and baroclinic terms, generally negligible in incompressible flows, are critical and play a key role in current under-expanded jets. The vorticity transport is not exclusively driven by vortex stretching but also by the compressibility and baroclinic effects.

The jets' self-similarity properties were also assessed. They can be estimated with the ratio of the radial penetration to the axial penetration. When the ratio is stable, it indicates that the jets reach a self-similarity [63].

Finally, Wu K. et al. focus on the simulation of the acoustic field of highly under-expanded jets to gain a deeper physical understanding of the noise generation mechanism [76].

6. Conclusions

In this review, a quick and, as far as possible, complete reference guide was presented in relation to the latest theoretical and experimental research activities regarding the investigation of under-expanded jets for application in advanced propulsion system.

Under-expanded jets are fluid flows that occur when a high-pressure fluid is suddenly released through a nozzle into a region of lower pressure. The term "under-expanded" specifically describes a condition where the fluid jet does not fully expand to match the surrounding pressure resulting in the formation of shock waves. Under-expanded jets are commonly encountered in various engineering applications, including rocket nozzles, gas and steam releases, supersonic exhaust from jet engines and during the injection of gaseous fuels in engine systems. Understanding the behaviour of under-expanded jets is now becoming crucial to develop clean and efficient combustion systems. For this reason, the most innovative experimental and numerical methods are used to study these jets.

Schlieren imaging is a broadly adopted technique for visualizing the overall jet development, and provides macroscopic information like jet penetration, cone angle, volume and morphology. Local measurements of the jet velocity and fuel density are also possible via exploiting other techniques like PLIF and PIV.

Fluid-dynamic simulation of under-expanded jets is an important field of research. In dealing with a compressible flow, special attention must be paid to choosing discretization schemes with low numerical diffusion while ensuring computational stability. High-order schemes, like ENO or WENO, provide a proficient representation of these flows types but require structured grids that offer little versatility. On the contrary, flux splitting methods (like KNP/KT or AUSM+), together with high-order integration schemes, are widely used with unstructured grids and provide very good results. However, the high-computational demands represent a significant drawback of these approaches. Grids on the order of magnitude of 10–50 μm are required. Depending on the thermodynamic conditions, a real gas equation of state may be required to adequately represent critical conditions or, more generally, deviation from the ideal gas behaviour.

Both outwardly and inwardly injection devices have been the topic of scientific research. The former category seems to be the best choice due to the amount of fuel they can supply in a relatively short period.

Injection pressure is usually of the order of tens of bar due to an evident limitation related to the fuel storage on-board. The injection usually occurs at ambient pressure, while nozzle holes are of the order of the millimetre.

The Mach disc is undoubtedly the most studied feature of under-expanded jets. It strongly affects the flow field, the air–fuel entrainment, and its geometrical features (width and height) are related to the pressure ratio. The Mach disc dimensions are usually of the order of magnitude of a few millimetres.

Turbulent mixing only occurs downstream of the Mach disc and the so-called potential core, typically extending 10/20 diameters downstream.

POD decomposition, Q-criterion surfaces and vorticity plots help understand turbulence characteristics, while scalar dissipation rate theory and statistical evaluation of the mixing activity provide relevant information regarding the air–fuel mixture formation.

Finally, it can be stated that the research efforts in investigating under-expanded jets in advanced propulsion systems will be further directed towards developing injection devices capable of supplying the required fuel amount in the strict timings available during the engine cycle. Experimental observations should deepen the jet morphology, providing further visualisations depicting especially quantitative parameters for comparison with CFD simulations. The numerical methods adopted for studying under-expanded jets are resource-demanding. So, optimised approaches should be developed to reduce the associated computational cost, mainly because these models are expected to be embedded in whole engine simulations.

Author Contributions: Conceptualization, F.D.; methodology, F.D.; data curation, F.D.; writing—original draft preparation, F.D.; supervision, C.V. and A.D.V.; writing—review and editing, C.V. and A.D.V. All authors have read and agreed to the published version of the manuscript.

Funding: This research received no external funding

Data Availability Statement: No new data were created or analyzed in this study. Data sharing is not applicable to this article.

Conflicts of Interest: The authors declare no conflicts of interest.

Abbreviations

The following abbreviations are used in this manuscript:

CFD	Computational Fluid Dynamics
CNG	Compressed Natural Gas
CVC	Constant Volume Chamber

DI	Direct Injection
DNS	Direct Numerical Simulation
fps	frames per second
ICE	Internal Combustion Engines
KNP	Kurganov
KT	Kurganov and Tadmor
LED	Light Emitting Diode
LES	Large Eddy Simulation
$\dot{m}^*$	critical mass flow
NPR	Net Pressure Ratio
PDF	Probability Density Function
PECU	Programmable Electronic Control Unit
PFI	Port Fuel Injected
P_{inj}	injection pressure
p_∞	ambient pressure
P^*	critical pressure
PISO	Pressure Implicit Split Operator
PPM	Piecewise Parabolic Method
RANS	Reynolds-Averaged Navier–Stokes
TKE	Turbulent Kinetic Energy
TTL	Transistor–Transistor Logic
WENO	Weighted Essentially Non-Oscillatory

References

1. Joshi, A. *Review of Vehicle Engine Efficiency and Emissions*; SAE Technical Papers; SAE International: Warrendale, PA, USA, 2020; Volume 2020; pp. 1–29. [CrossRef]
2. IPCC. *Climate Change 2021: The Physical Science Basis. Contribution of Working Group I to the Sixth Assessment Report of the Intergovernmental Panel on Climate Change*; Masson-Delmotte, V., Zhai, P., Pirani, A., Connors, S.L., Péan, C., Berger, S., Caud, N., Chen, Y., Eds.; Cambridge University Press: Cambridge, UK, 2021; p. 3949.
3. International Energy Agency. *Tracking Transport 2020*; IEA: Paris, France, 2021.
4. International Energy Agency. *Net Zero by 2050: A Roadmap for the Global Energy Sector*; IEA: Paris, France, 2021; p. 224.
5. Li, F.; Wang, Z.; Wang, Y.; Wang, B. High-Efficiency and Clean Combustion Natural Gas Engines for Vehicles. *Automot. Innov.* **2019**, *2*, 284–304. [CrossRef]
6. Senecal, K.; Leach, F. *Racing Toward Zero: The Untold Story of Driving Green*; SAE International: Warrendale, PA, USA, 2021.
7. Sankesh, D.; Lappas, P. *Natural-Gas Direct-Injection for Spark-Ignition Engines—A Review on Late-Injection Studies*; SAE International: Warrendale, PA, USA, 2018. [CrossRef]
8. Nocivelli, L.; Sforzo, B.A.; Tekawade, A.; Yan, J.; Powell, C.F.; Chang, W.; Lee, C.F.; Som, S. *Analysis of the Spray Numerical Injection Modeling for Gasoline Applications*; SAE Technical Papers; SAE International: Warrendale, PA, USA, 2020. [CrossRef]
9. Zembi, J.; Mariani, F.; Battistoni, M.; Irimescu, A.; Merola, S. Numerical Investigation of Water Injection Effects on Flame Wrinkling and Combustion Development in a GDI Spark Ignition Optical Engine. In Proceedings of the SAE WCX Digital Summit, Virtual, 12–15 April 2021; SAE International: Warrendale, PA, USA, 2021. [CrossRef]
10. Oh, H.; Hwang, J.; Pickett, L.M.; Han, D. Machine-learning based prediction of injection rate and solenoid voltage characteristics in GDI injectors. *Fuel* **2022**, *311*, 122569. [CrossRef]
11. Allocca, L.; Montanaro, A.; Meccariello, G.; Duronio, F.; Ranieri, S.; De Vita, A. *Under-Expanded Gaseous Jets Characterization for Application in Direct Injection Engines: Experimental and Numerical Approach*; SAE Technical Papers; SAE International: Warrendale, PA, USA, 2020; Volume 2020; pp. 1–15. [CrossRef]
12. Yip, H.L.; Srna, A.; Chun, A.; Yuen, A.C.Y.; Kook, S.; Taylor, R.; Yeoh, G.; Medwell, P.; Chan, Q. A Review of Hydrogen Direct Injection for Internal Combustion Engines: Towards Carbon-Free Combustion. *Appl. Sci.* **2019**, *9*, 4842. [CrossRef]
13. Hajialimohammadi, A.; Honnery, D.; Abdullah, A.; Mirsalim, M.A. Time resolved characteristics of gaseous jet injected by a group-hole nozzle. *Fuel* **2013**, *113*, 497–505. [CrossRef]
14. Chiodi, M.; Berner, H.J.; Bargende, M. *Investigation on Different Injection Strategies in a Direct-Injected Turbocharged Cng-Engine*; SAE Technical Papers; SAE International: Warrendale, PA, USA, 2006. [CrossRef]
15. Yadollahi, B.; Boroomand, M. The effect of combustion chamber geometry on injection and mixture preparation in a CNG direct injection SI engine. *Fuel* **2013**, *107*, 52–62. [CrossRef]
16. Erfan, I.; Hajialimohammadi, A.; Chitsaz, I.; Ziabasharhagh, M.; Martinuzzi, R.J. Influence of chamber pressure on CNG jet characteristics of a multi-hole high pressure injector. *Fuel* **2017**, *197*, 186–193. [CrossRef]
17. Duronio, F.; Ranieri, S.; Montanaro, A.; Allocca, L.; De Vita, A. ECN Spray G injector: Numerical modelling of flash-boiling breakup and spray collapse. *Int. J. Multiph. Flow* **2021**, *145*, 103817. [CrossRef]
18. Fox, J.H. On the Structure of Jet Plumes. *AIAA J.* **1974**, *12*, 105–107. [CrossRef]

19. Doroudi, S. *Ansys Fluent Modelling of an Underexpanded Supersonic Sootblower Jet Impinging into Recovery Boiler Tube Geometries*; University of Toronto (Canada): Toronto, ON, Canada, 2015.
20. Knowles, K.; Saddington, A.J. A review of jet mixing enhancement for aircraft propulsion applications. *Proc. Inst. Mech. Eng. Part G J. Aerosp. Eng.* **2006**, *220*, 103–127. [CrossRef]
21. Orescanin, M.M.; Austin, J.M.; Kieffer, S.W. Unsteady high-pressure flow experiments with applications to explosive volcanic eruptions. *J. Geophys. Res. Solid Earth* **2010**, *115*. [CrossRef].
22. Von der Linden, J.; Kimblin, C.; McKenna, I.; Bagley, S.; Li, H.C.; Houim, R.; Kueny, C.S.; Kuhl, A.; Grote, D.; Converse, M.; et al. Standing shock prevents propagation of sparks in supersonic explosive flows. *Commun. Earth Environ.* **2021**, *2*, 195. [CrossRef]
23. Carcano, S.; Bonaventura, L.; Esposti Ongaro, T.; Neri, A. A semi-implicit, second-order-accurate numerical model for multiphase underexpanded volcanic jets. *Geosci. Model Dev.* **2013**, *6*, 1905–1924. [CrossRef]
24. Verhelst, S. Recent progress in the use of hydrogen as a fuel for internal combustion engines. *Int. J. Hydrogen Energy* **2014**, *39*, 1071–1085. . [CrossRef]
25. Onorati, A.; Payri, R.; Vaglieco, B.; Agarwal, A.; Bae, C.; Bruneaux, G.; Canakci, M.; Gavaises, M.; Günthner, M.; Hasse, C.; et al. The role of hydrogen for future internal combustion engines. *Int. J. Engine Res.* **2022**, *23*, 529–540. [CrossRef]
26. Kurnia, J.C.; Sasmito, A.P., Hydrogen Fuel Cell in Vehicle Propulsion: Performance, Efficiency, and Challenge. In *Energy Efficiency in Mobility Systems*; Sulaiman, S.A., Ed.; Springer: Singapore, 2020; pp. 9–26. [CrossRef]
27. Petrescu, R.V.V.; Machín, A.; Fontánez, K.; Arango, J.C.; Márquez, F.M.; Petrescu, F.I.T. Hydrogen for aircraft power and propulsion. *Int. J. Hydrogen Energy* **2020**, *45*, 20740–20764. [CrossRef]
28. Depcik, C.; Cassady, T.; Collicott, B.; Burugupally, S.P.; Li, X.; Alam, S.S.; Arandia, J.R.; Hobeck, J. Comparison of lithium ion Batteries, hydrogen fueled combustion Engines, and a hydrogen fuel cell in powering a small Unmanned Aerial Vehicle. *Energy Convers. Manag.* **2020**, *207*, 112514. [CrossRef]
29. Abdel-Rahman, A. A review of effects of initial and boundary conditions on turbulent jets. *WSEAS Trans. Fluid Mech.* **2010**, *4*, 257–275.
30. Donaldsion, C.; Snedeker, R. A study of free jet impingement. *J. Fluid Mech.* **1971**, *45*, 281–319. [CrossRef]
31. Saddington, A.J.; Lawson, N.J.; Knowles, K. An experimental and numerical investigation of under-expanded turbulent jets. *Aeronaut. J.* **2004**, *108*, 145–152. [CrossRef]
32. John, J. *Gas Dynamics*; Prentice Hall PTR: Hoboken, NJ, USA, 1984.
33. Dam, N.J.; Rodenburg, M.; Tolboom, R.A.L.; Stoffels, G.G.M.; Huisman-Kleinherenbrink, P.M.; ter Meulen, J.J. Imaging of an underexpanded nozzle flow by UV laser Rayleigh scattering. *Exp. Fluids* **1998**, *24*, 93–101. [CrossRef]
34. Saad, M. *Compressible Fluid Flow*; Prentice-Hall: Hoboken, NJ, USA, 1985.
35. EWAN, B.C.R.; MOODIE, K. Structure and Velocity Measurements in Underexpanded Jets. *Combust. Sci. Technol.* **1986**, *45*, 275–288. [CrossRef]
36. Keith, T.G.; John, J.E. *Gas Dynamics*; Pearson Education, Inc.: Upper Saddle River, NJ, USA, 2006.
37. Zucker, R.D.; Biblarz, O. *Fundamentals of Gas Dynamics*; John Wiley & Sons: Hoboken, NJ, USA, 2002.
38. Antsupov, A. Properties of Underexpanded and Overexpanded Supersonic Gas Jets. *Sov. Phys. Tech. Phys.* **1974**, *19*, 234 – 238.
39. Hatanaka, K.; Saito, T. Influence of nozzle geometry on underexpanded axisymmetric free jet characteristics. *Shock Waves* **2012**, *22*, 427–434. [CrossRef]
40. Addy, A.L. Effects of axisymmetric sonic nozzle geometry on Mach disk characteristics. *AIAA J.* **1981**, *19*, 121–122. [CrossRef]
41. Dong, Q.; Li, Y.; Song, E.; Fan, L.; Yao, C.; Sun, J. Visualization research on injection characteristics of high-pressure gas jets for natural gas engine. *Appl. Therm. Eng.* **2018**, *132*, 165–173. [CrossRef]
42. Zhao, J.; Liu, W.; Liu, Y. Experimental investigation on the microscopic characteristics of underexpanded transient hydrogen jets. *Int. J. Hydrogen Energy* **2020**, *45*, 16865–16873. [CrossRef]
43. Ni, Z.; Dong, Q.; Wang, D.; Yang, X. Visualization research of natural gas jet characteristics with ultra-high injection pressure. *Int. J. Hydrogen Energy* **2022**, *47*, 32473–32492. [CrossRef]
44. Settles, G.S. *Schlieren and Shadowgraph Techniques: Visualizing Phenomena in Transparent Media*; Springer Science & Business Media: Berlin/Heidelberg, Germany, 2001.
45. Panigrahi, P.K.; Muralidhar, K. *Schlieren and Shadowgraph Methods in Heat and Mass Transfer*; Springer: Berlin/Heidelberg, Germany, 2012; Volume 2.
46. Kook, S.; Le, M.K.; Padala, S.; Hawkes, E.R. Z-type Schlieren Setup and its Application to High-Speed Imaging of Gasoline Sprays. In Proceedings of the SAE International Powertrains, Fuels and Lubricants Meeting, Kyoto, Japan, 30 August–2 September 2011; SAE International: Warrendale, PA, USA, 2011. [CrossRef]
47. Montanaro, A.; Allocca, L.; De Vita, A.; Ranieri, S.; Duronio, F.; Meccariello, G. Experimental and Numerical Characterization of High-Pressure Methane Jets for Direct Injection in Internal Combustion Engines. In Proceedings of the SAE Powertrains, Fuels & Lubricants Meeting, Kraków, Poland, 22–24 September, 2020; SAE International: Warrendale, PA, USA, 2020. [CrossRef]
48. Samsam-Khayani, H.; Chen, B.; Kim, M.; Kim, K.C. Visualization of supersonic free jet flow structures subjected to various temperature and pressure ratio conditions. *Opt. Lasers Eng.* **2022**, *158*, 107144. [CrossRef]
49. Yu, J.; Hillamo, H.; Vuorinen, V.; Sarjovaara, T.; Kaario, O.; Larmi, M. *Experimental Investigation of Characteristics of Transient Low Pressure Wall-Impinging Gas Jet*; Institute of Physics Publishing: Bristol, UK, 2011; Volume 318. [CrossRef]

50. Yu, J.; Vuorinen, V.; Kaario, O.; Sarjovaara, T.; Larmi, M. Visualization and analysis of the characteristics of transitional underexpanded jets. *Int. J. Heat Fluid Flow* **2013**, *44*, 140–154. [CrossRef]
51. Sakellarakis, V.D.; Vera-Tudela, W.; Doll, U.; Ebi, D.; Wright, Y.M.; Boulouchos, K. The effect of high-pressure injection variations on the mixing state of underexpanded methane jets. *Int. J. Engine Res.* **2021**, *22*, 2900–2918. [CrossRef]
52. Deshmukh, A.Y.; Falkenstein, T.; Pitsch, H.; Khosravi, M.; van Bebber, D.; Klaas, M.; Schroeder, W. Numerical Investigation of Direct Gas Injection in an Optical Internal Combustion Engine. *SAE Int. J. Engines* **2018**, *11*, 353–378. [CrossRef]
53. Yu, J.; Vuorinen, V.; Kaario, O.; Sarjovaara, T.; Larmi, M. Characteristics of High Pressure Jets for Direct Injection Gas Engine. *Int. J. Fuels Lubr.* **2013**, *6*, 149–156. [CrossRef]
54. Schulz, C.; Sick, V. Tracer-LIF diagnostics: Quantitative measurement of fuel concentration, temperature and fuel/air ratio in practical combustion systems. *Prog. Energy Combust. Sci.* **2005**, *31*, 75–121. [CrossRef]
55. Kirchweger, W.; Haslacher, R.; Hallmannsegger, M.; Gerke, U. Applications of the LIF method for the diagnostics of the combustion process of gas-IC-engines. *Exp. Fluids* **2007**, *43*, 329–340. [CrossRef]
56. Banholzer, M.; Vera-Tudela, W.; Traxinger, C.; Pfitzner, M.; Wright, Y.; Boulouchos, K. Numerical investigation of the flow characteristics of underexpanded methane jets. *Phys. Fluids* **2019**, *31*, 056105. [CrossRef]
57. Thawko, A.; van Hout, R.; Yadav, H.; Tartakovsky, L. Flow field characteristics of a confined, underexpanded transient round jet. *Phys. Fluids* **2021**, *33*. [CrossRef]
58. Xiao, C.N.; Fond, B.; Beyrau, F.; T'Joen, C.; Henkes, R.; Veenstra, P.; van Wachem, B. Numerical Investigation and Experimental Comparison of the Gas Dynamics in a Highly Underexpanded Confined Real Gas Jet. *Flow Turbul. Combust.* **2019**, *103*, 141–173. [CrossRef]
59. Duronio, F.; Mascio, A.D.; Villante, C.; Anatone, M.; Vita, A.D. ECN Spray G: Coupled Eulerian internal nozzle flow and Lagrangian spray simulation in flash boiling conditions. *Int. J. Engine Res.* **2023**, *24*, 1530–1544. [CrossRef]
60. Hamzehloo, A.; Aleiferis, P.G. Large Eddy Simulation of Near-Nozzle Shock Structure and Mixing Characteristics of Hydrogen Jets for Direct-Injection Spark-Ignition Engines. In Proceedings of the 10th International Conference on Heat Transfer, Fluid Mechanics and Thermodynamics, Orlando, FL, USA, 14–16 July 2014.
61. Rahantamialisoa, F.N.; Zembi, J.; Miliozzi, A.; Sahranavardfard, N.; Battistoni, M. *CFD Simulations of Under-Expanded Hydrogen Jets under High-Pressure Injection Conditions*; Institute of Physics: Bristol, UK, 2022; Volume 2385. [CrossRef]
62. Verrière, J.; Kopriva, J.E. *Simulations of an Underexpanded Round Jet Using the Lattice-Boltzmann Method*; American Institute of Aeronautics and Astronautics Inc.: Reston, VA, USA, 2021. [CrossRef]
63. Kopriva, J.E.; Laskowski, G.M.; Polidoro, F.; Li, Y.; Jammalamadaka, A.; Nardari, C. *Lattice-Boltzmann Simulations of an Underexpanded Jet from a Rectangular Nozzle with and without Aft-Deck*; American Institute of Aeronautics and Astronautics Inc.: Reston, VA, USA, 2019. [CrossRef]
64. Ren, Z.; Wen, J.X. Numerical characterization of under-expanded cryogenic hydrogen gas jets. *AIP Adv.* **2020**, *10*. [CrossRef]
65. Buttay, R.; Lehnasch, G.; Mura, A. Analysis of small-scale scalar mixing processes in highly under-expanded jets. *Shock Waves* **2016**, *26*, 193–212. [CrossRef]
66. Quimby, D.; Jacobs, G.B. *Large Eddy Simulation of a Supersonic Underexpanded Jet with a High-Order Hybrid WENO-Z/central Scheme*; American Institute of Aeronautics and Astronautics Inc.: Reston, VA, USA, 2016. [CrossRef]
67. Su, H.; Cai, J.; Qu, K.; Pan, S. Numerical simulations of inert and reactive highly underexpanded jets. *Phys. Fluids* **2020**, *32*. [CrossRef]
68. Greenshields, C.J.; Weller, H.G.; Gasparini, L.; Reese, J.M. Implementation of semi-discrete, non-staggered central schemes in a colocated, polyhedral, finite volume framework, for high-speed viscous flows. *Int. J. Numer. Methods Fluids* **2010**, *63*, 1–21. [CrossRef]
69. Versteg, H.; Malalasekera, W. *An introduction to Computational Fluid Dynamics: The Finite Volume Method*, 2nd ed.; Pearson Education: London, UK, 2007.
70. Di Angelo, L.; Duronio, F.; De Vita, A.; Di Mascio, A. Cartesian Mesh Generation with Local Refinement for Immersed Boundary Approaches. *J. Mar. Sci. Eng.* **2021**, *9*, 572. [CrossRef]
71. Kurganov, A.; Tadmor, E. New High-Resolution Central Schemes for Nonlinear Conservation Laws and Convection-Diffusion Equations. *J. Comput. Phys.* **2000**, *160*, 241–282. [CrossRef]
72. Kurganov, A.; Noelle, S.; Petrova, G. Semidiscrete Central-Upwind Schemes for Hyperbolic Conservation Laws and Hamilton–Jacobi Equations. *SIAM J. Sci. Comput.* **2001**, *23*, 707–740. [CrossRef]
73. van Leer, B. Towards the ultimate conservative difference scheme. II. Monotonicity and conservation combined in a second-order scheme. *J. Comput. Phys.* **1974**, *14*, 361–370. [CrossRef]
74. Jin, Y.; Yao, W. *LES Investigation of Real-Fluid Effect on Underexpanded Jets*; American Institute of Aeronautics and Astronautics Inc.: Reston, VA, USA, 2021. [CrossRef]
75. Duronio, F.; Montanaro, A.; Ranieri, S.; Allocca, L.; De Vita, A. Under-Expanded Jets Characterization by Means of CFD Numerical Simulation Using an Open FOAM Density-Based Solver. In Proceedings of the 15th International Conference on Engines & Vehicles, Napoli, Italy, 12–16 September 2021; SAE International: Warrendale, PA, USA, 2021. [CrossRef]
76. Wu, K.; Li, X.; Yao, W.; Fan, X. *Three-Dimensional Numerical Study of the Acoustic Properities of a Highly Underexpanded Jet*; AIAA American Institute of Aeronautics and Astronautics: Reston, VA, USA, 2015. [CrossRef]

77. Li, X.; Yao, W.; Fan, X. Large-eddy simulation of time evolution and instability of highly underexpanded sonic jets. *AIAA J.* **2016**, *54*, 3191–3211. [CrossRef]
78. Vuorinen, V.; Wehrfritz, A.; Yu, J.; Kaario, O.; Larmi, M.; Boersma, B.J. Large-eddy simulation of subsonic jets. *J. Phys. Conf. Ser.* **2011**, *318*, 032052. [CrossRef]
79. Vuorinen, V.; Keskinen, J.P.; Duwig, C.; Boersma, B.J. On the implementation of low-dissipative Runge–Kutta projection methods for time dependent flows using OpenFOAM®. *Comput. Fluids* **2014**, *93*, 153–163. [CrossRef]
80. Vuorinen, V.; Larmi, M.; Schlatter, P.; Fuchs, L.; Boersma, B.J. A low-dissipative, scale-selective discretization scheme for the Navier–Stokes equations. *Comput. Fluids* **2012**, *70*, 195–205. [CrossRef]
81. Modesti, D.; Pirozzoli, S. A low-dissipative solver for turbulent compressible flows on unstructured meshes, with OpenFOAM implementation. *Comput. Fluids* **2017**, *152*, 14–23. [CrossRef]
82. Hamzehloo, A.; Aleiferis, P.G. Numerical modelling of transient under-expanded jets under different ambient thermodynamic conditions with adaptive mesh refinement. *Int. J. Heat Fluid Flow* **2016**, *61*, 711–729. [CrossRef]
83. Sun, G.; Wu, G.; Liu, C.J. Numerical Simulation of Supersonic Flow with Shock Wave using Modified AUSM Scheme. *Int. J. Nonlinear Sci. Numer. Simul.* **2006**, *7*, 329–332. [CrossRef]
84. Vuorinen, V.; Wehrfritz, A.; Duwig, C.; Boersma, B.J. Large-eddy simulation on the effect of injection pressure and density on fuel jet mixing in gas engines. *Fuel* **2014**, *130*, 241–250. [CrossRef]
85. Vuorinen, V.; Yu, J.; Tirunagari, S.; Kaario, O.; Larmi, M.; Duwig, C.; Boersma, B.J. Large-eddy simulation of highly underexpanded transient gas jets. *Phys. Fluids* **2013**, *25*, 016101. [CrossRef]
86. Hamzehloo, A.; Aleiferis, P.G. LES and RANS modelling of under-expanded jets with application to gaseous fuel direct injection for advanced propulsion systems. *Int. J. Heat Fluid Flow* **2019**, *76*, 309–334. [CrossRef]
87. Deshmukh, A.Y.; Bode, M.; Pitsch, H.; Khosravi, M.; Bebber, D.v.; Vishwanathan, G. Characterization of Hollow Cone Gas Jets in the Context of Direct Gas Injection in Internal Combustion Engines. *SAE Int. J. Fuels Lubr.* **2018**, *11*, 353–377. [CrossRef]
88. Bartolucci, L.; Cordiner, S.; Mulone, V.; Rocco, V. Natural Gas Stable Combustion under Ultra-Lean Operating Conditions in Internal Combustion Engines. *Energy Procedia* **2016**, *101*, 886–892. [CrossRef]
89. Hamzehloo, A.; Aleiferis, P. Large eddy simulation of highly turbulent under-expanded hydrogen and methane jets for gaseous-fuelled internal combustion engines. *Int. J. Hydrogen Energy* **2014**, *39*, 21275–21296. [CrossRef]
90. De Vita, M.; Duronio, F.; De Vita, A.; De Berardinis, P. Adaptive Retrofit for Adaptive Reuse: Converting an Industrial Chimney into a Ventilation Duct to Improve Internal Comfort in a Historic Environment gas expansion. *Sustainability* **2022**, *14* 3360. [CrossRef]
91. Zhu, H.; Battistoni, M.; Manjegowda Ningegowda, B.; Nadia Zazaravaka Rahantamialisoa, F.; Yue, Z.; Wang, H.; Yao, M. Thermodynamic modeling of trans/supercritical fuel sprays in internal combustion engines based on a generalized cubic equation of state. *Fuel* **2022**, *307*, 121894. [CrossRef]
92. Li, X.; Zhou, R.; Yao, W.; Fan, X. Flow characteristic of highly underexpanded jets from various nozzle geometries. *Appl. Therm. Eng.* **2017**, *125*, 240–253. [CrossRef]
93. Anaclerio, G.; Capurso, T.; Torresi, M.; Camporeale, S.M. *Numerical Characterization of Hydrogen Under-Expanded Jets: Influence of the Nozzle Cross-Section Shape*; Institute of Physics: Bristol, UK, 2022, Volume 2385. [CrossRef]
94. Bonelli, F.; Viggiano, A.; Magi, V. A numerical analysis of hydrogen underexpanded jets under real gas assumption. *J. Fluids Eng. Trans. ASME* **2013**, *135*. [CrossRef]
95. Kaario, O.; Vuorinen, V.; Hulkkonen, T.; Keskinen, K.; Nuutinen, M.; Larmi, M.; Tanner, F.X. Large eddy simulation of high gas density effects in fuel sprays. *At. Sprays* **2013**, *23*, 297–325. [CrossRef]
96. Pope, S.B. *Turbulent Flows*; Cambridge University Press: Cambridge, UK, 2001.
97. Weickert, M.; Teike, G.; Schmidt, O.; Sommerfeld, M. Investigation of the LES WALE turbulence model within the lattice Boltzmann framework. *Comput. Math. Appl.* **2010**, *59*, 2200–2214. [CrossRef]
98. Huang, S.; Li, Q.S. A new dynamic one-equation subgrid-scale model for large eddy simulations. *Int. J. Numer. Methods Eng.* **2010**, *81*, 835–865.
99. Yoshizawa, A; Horiuti, K. A statistically-derived subgrid-scale kinetic energy model for the large-eddy simulation of turbulent flows. *J. Phys. Soc. Jpn.* **1985**, *54*, 2834–2839. [CrossRef]
100. Munday, D.; Gutmark, E.; Liu, J.; Kailasanath, K. Flow structure and acoustics of supersonic jets from conical convergent-divergent nozzles. *Phys. Fluids* **2011**, *23*, 116102,
101. Garnier, E.; Adams, N.; Sagaut, P. *Large Eddy Simulation for Compressible Flows*; Springer Science & Business Media: Berlin/Heidelberg, Germany, 2009.
102. Rana, Z.A.; Thornber, B.; Drikakis, D. Transverse jet injection into a supersonic turbulent cross-flow. *Phys. Fluids* **2011**, *23*, 046103.
103. Hamzehloo, A.; Aleiferis, P.G. Gas dynamics and flow characteristics of highly turbulent under-expanded hydrogen and methane jets under various nozzle pressure ratios and ambient pressures. *Int. J. Hydrogen Energy* **2016**, *41*, 6544–6566. [CrossRef]
104. Duronio, F.; Ranieri, S.; Mascio, A.D.; Vita, A.D. Simulation of high pressure, direct injection processes of gaseous fuels by a density-based OpenFOAM solver. *Phys. Fluids* **2021**, *33*, 066104.
105. Duronio, F.; Montanaro, A.; Allocca, L.; Ranieri, S.; De Vita, A. Effects of Thermodynamic Conditions and Nozzle Geometry in Gaseous Fuels Direct Injection Process for Advanced Propulsion Systems. In Proceedings of the WCX SAE World Congress Experience, Detroit, MI, USA, 18–20 April 2020; SAE International: Warrendale, PA, USA, 2022. [CrossRef]

106. Banholzer, M.; Müller, H.; Pfitznery, M. *Numerical Investigation of the Flow Structure of Underexpanded Jets in Quiescent Air Using Real-Gas Thermodynamics*; American Institute of Aeronautics and Astronautics Inc.: Reston, VA, USA, 2017. [CrossRef]
107. Traxinger, C.; Banholzer, M.; Pfitzner, M. Real-Gas Effects and Phase Separation in Underexpanded Jets at Engine-Relevant Conditions. In Proceedings of the 2018 AIAA Aerospace Sciences Meeting, Kissimmee, FL, USA, 8–12 January 2018. [CrossRef]
108. Rahantamialisoa, F.; Battistoni, M.; Miliozzi, A.; Sahranavardfard, N.; Zembi, J. *Investigations on Hydrogen Injections Using a Real-Fluid Approach*; SAE International: Warrendale, PA, USA, 2023. [CrossRef]
109. Yosri, M.R.; Talei, M.; Gordon, R.; Brear, M.; Lacey, J. *A Numerical Simulation of an Under-Expanded Jet Issued from a Prototype Injector*; The University of Queensland: Brisbane, Australia, 2020. [CrossRef]
110. Bartolucci, L.; Cordiner, S.; Mulone, V.; Scarcelli, R.; Wallner, T.; Swantek, A.; Powell, C.; Kastengren, A. Gaseous jet through an outward opening injector: Details of mixing characteristic and turbulence scales. *Int. J. Heat Fluid Flow* **2020**, *85*, 108660. [CrossRef]
111. Cao, W.; Zhou, Z.; Zhou, W.; Xu, S.; Xiao, Q.; Cao, W.; Jiao, F.; Zhang, Y.; Yu, S.; Xu, S. The flow field behaviours of under-expansion jet flame in premixed hydrogen/air explosion venting. *Int. J. Hydrogen Energy* **2022**, *47*, 10420–10430. [CrossRef]
112. Duronio, F.; Di Mascio, A.; De Vita, A.; Innocenzi, V.; Prisciandaro, M. Eulerian–Lagrangian modeling of phase transition for application to cavitation-driven chemical processes. *Phys. Fluids* **2023**, *35*, 053305.
113. Förster, F.J.; Baab, S.; Steinhausen, C.; Lamanna, G.; Ewart, P.; Weigand, B. Mixing characterization of highly underexpanded fluid jets with real gas expansion. *Exp. Fluids* **2018**, *59*. [CrossRef]
114. Verhelst, S.; Sierens, R. Hydrogen engine-specific properties. *Int. J. Hydrogen Energy* **2001**, *26*, 987–990. [CrossRef]

Disclaimer/Publisher's Note: The statements, opinions and data contained in all publications are solely those of the individual author(s) and contributor(s) and not of MDPI and/or the editor(s). MDPI and/or the editor(s) disclaim responsibility for any injury to people or property resulting from any ideas, methods, instructions or products referred to in the content.